Inorganic Chemistry

Article

pubs.acs.org/IC

Theory of Late-Transition-Metal Alkyl and Heteroatom Bonding: Analysis of Pt, Ru, Ir, and Rh Complexes

Deepa Devarajan,[†] T. Brent Gunnoe,[‡] and Daniel H. Ess*[,†,§]

[†]Department of Chemistry and Biochemistry, Brigham Young University, Provo, Utah 84602, United States

[‡]Department of Chemistry, University of Virginia, Charlottesville, Virginia 22904, United States

Supporting Information

ABSTRACT: Density functional and correlated ab initio methods were used to calculate, compare, and analyze bonding interactions in late-transition-metal alkyl and heteroatom complexes (M−X). The complexes studied include: (DMPE)Pt(CH_3)(X) (DMPE = 1,2-bis(dimethylphosphino)ethane), Cp*Ru(PMe_3)$_2$(X) (Cp* = pentamethylcyclopentadienyl), (DMPE)$_2$Ru(H)(X), (Tp)(CO)Ru(Py)(X) (Tp = trispyrazolylborate), (PMe_3)$_2$Rh(C_2H_4)-(X), and *cis*-(acac)$_2$Ir(Py)(X) (acac = acetylacetonate). Seventeen X ligands were analyzed that include alkyl (CR_3), amido (NR_2), alkoxo (OR), and fluoride. Energy decomposition analysis of these M−X bonds revealed that orbital charge transfer stabilization provides a straightforward model for trends in bonding along the alkyl to heteroatom ligand series (X = CH_3, NH_2, OH, F). Pauli repulsion (exchange repulsion), which includes contributions from closed-shell d_π-p_π repulsion, generally decreases along the alkyl to heteroatom ligand series but depends on the exact M−X complexes. It was also revealed that stabilizing electrostatic interactions generally decrease along this ligand series. Correlation between M−X and H−X bond dissociation energies is good with R^2 values between 0.7 and 0.9. This correlation exists because for both M−X and H−X bonds the orbital stabilization energies are a function of the orbital electronegativity of the X group. The greater than 1 slope when correlating M−X and H−X bond dissociation energies was traced back to differences in Pauli repulsion and electrostatic stabilization.

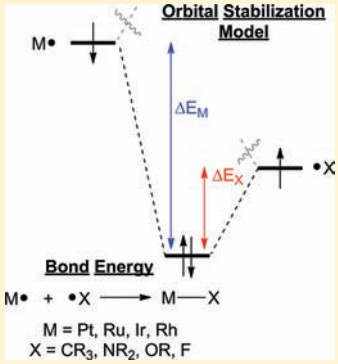

INTRODUCTION

Recently there has been a surge in the synthesis of complexes that possess metal heteroatom bonds.[1] Some examples include Gunnoe and Cundari's TpRu(L)(X) (X = CH_3, OR, and NR_2; Tp = hydridotris(pyrazolyl)borate),[2] (PCP)Ru(CO)(NH_2) (PCP = 1,3-bis[(di-*tert*-butylphosphino)methyl]-2,4,6-trimethylbenzene),[3] and (^{t}bpy)Pt(NHPh)(Me) (^{t}bpy =4,4′-di-*tert*-butyl-2,2′-dipyridyl) complexes,[4] Periana and Goddard's *cis*-(acac)$_2$Ir(L)(X) (X = Ph, OMe; acac = acetylacetonate; L = pyridine or MeOH) complexes,[5] Goldberg's (PNP)Rh(OR) (PNP = 2,6-bis[di-*tert*-butylphosphino)methyl]pyridine, R = H, Ph) complex,[6] Labinger and Bercaw's [(diimine)M(μ-OH)]$_2^{2+}$ (M = Pd, Pt) and [(COD)Rh(μ_2-OH)]$_2$ complexes,[7] and Bergman's Cp*(PPh_3)Ir(OEt)(H), Cp*(PMe_3)Ir(OH)(Ph), Cp*(PMe_3)Ir(H)(NH_2), and (DMPE)$_2$M(H)(NH_2) (M = Ru, Fe) complexes.[8] Because of this increased interest in metal heteroatom complexes, our group recently used density functional methods to investigate whether there is an advantage to utilize metal amido (M−NR_2) or metal alkoxo (M−OR) complexes, compared with metal alkyl (M−R) complexes, to activate hydrocarbon C−H bonds.[9] We found that ground-state effects such as the donor capacity of the heteroatom group to labilize a ligand and the cis ligand effect[10] are more important than transition-state effects. We have now turned our attention to understanding the nature of bonding and properties of M−X bonds where X = alkyl, amido, alkoxo, fluoride, and related ligands.

Metal heteroatom bonding in late-transition-metal complexes has been thought to be less ionic, to have a hard-soft mismatch, and to be weaker than metal heteroatom bonding in early transition-metal counterparts.[11] In addition, it has been suggested that d_π-p_π repulsion interactions are the source of many differences between late-transition-metal heteroatom bonding and early transition-metal heteroatom bonding (Scheme 1). For example, Caulton has suggested that d_π-p_π repulsion is a factor contributing to the relatively low bond strengths for ruthenium alkoxide and ruthenium amide bonds in Cp*Ru(PMe_3)$_2$(X) complexes.[12] In addition, d_π-p_π repulsion has been invoked as an important property in a variety of other late-transition-metal complexes. For example, Perutz and co-workers have recently suggested that d_π-p_π repulsion is important for the reactivity and thermodynamics of M−F bonding in Ni and Pt complexes.[13]

d_π-p_π Repulsion arises from a four-electron, two-orbital interaction between a ligand lone pair and a filled d orbital as a consequence of enforcing an antisymmetrized wave function description to comply with the Pauli exclusion principle. This type of repulsion is often termed closed-shell repulsion. This π-type interaction has been proposed to reduce thermodynamic stability and increase reactivity of these complexes by including nucleophilicity and basicity.[12,14]

Received: February 16, 2012
Published: June 4, 2012

   dx.doi.org/10.1021/ic300350k | *Inorg. Chem.* 2012, 51, 6710−6718

Scheme 1. Closed-Shell Orbital Interaction Diagram Depicting d_π-p_π Repulsions in Late-Transition-Metal Heteroatom Complexes

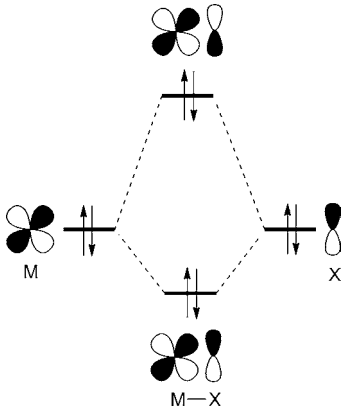

There remains doubt about whether π repulsion is necessary to explain the stability and/or reactivity of late-transition-metal heteroatom complexes.[15] In 1987, Bryndza, Bercaw, and co-workers reported exchange equilibria for (DPPE)Pt(CH_3)(OMe) (DPPE = 1,2-bis(diphenylphosphino)ethane) and Cp*Ru(PMe_3)$_2$(OH) complexes with H−Y (Y = OR and NR_2) species (eq 1−2).[16] For the (DPPE)Pt(CH_3)(OMe) complex, studies of equilibration with H−Y = HOH, $HNPh_2$, HNMePh, and H_3CCOCH_3 (eq 1) revealed K_{eq} values close to 1. Similarly, the equilibrium between Cp*Ru(PMe_3)$_2$(OH) and H−Y = H_2NPh, HNMePh, and H_3CCOCH_3 gave K_{eq} values of ∼1. Importantly, these equilibrium constants showed negligible solvent dependence. In addition, the K_{eq} values were demonstrated to be close to 1 because of small changes in enthalpy and entropy rather than enthalpy−entropy cancellation. These studies suggested that the difference between H−X and H−Y bond dissociation energies (BDEs) is the same as the difference between M−X and M−Y BDEs. Plotting absolute H−X BDE values with relative M−X BDEs gave a highly correlated linear relationship suggesting that d_π-p_π repulsion may not control M−X bonding or may be relatively constant between different complexes. Bergman and co-workers have conducted similar studies.[8,17]

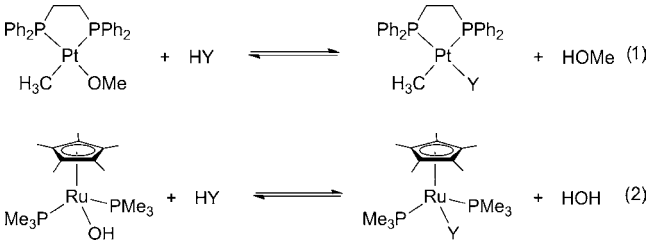

The varied opinions about the relative nature of M−X bonding led Hartwig to remark that the origin of the strengths of late-metal alkoxides and amides remains unresolved.[18] In order to help bring clarity to this topic, we have now used density functional and correlated ab initio methods to calculate, compare, and dissect bond energies (BEs)[19] for late-transition-metal alkyl and heteroatom complexes that include (DMPE)-Pt(CH_3)(X) **1−X**, Cp*Ru(PMe_3)$_2$(X) **2−X**, (DMPE)$_2$Ru(H)-(X) **3−X**, (PMe_3)$_2$Rh(C_2H_4)(X) **4−X**, (Tp)(CO)Ru(Py)(X) **5−X**, and *cis*-(acac)$_2$Ir(Py)(X) **6−X** (X = CR_3, NR_2, OR, and F, Scheme 2). We have also investigated the origin of correlation between M−X and H−X bond dissociation energies.

Scheme 2. Complexes Studied for X = CR_3, NR_2, OR, and F

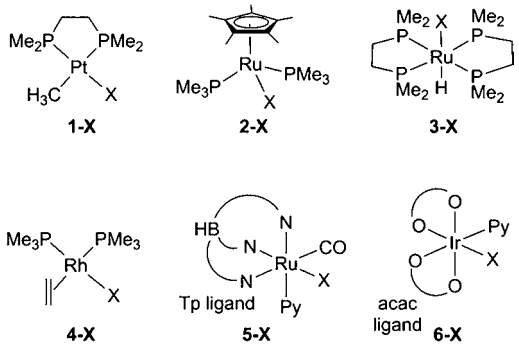

BACKGROUND

Although there are numerous reports of experimentally determined metal carbon bond energies,[20] there are relatively few reports probing the origin of metal alkyl or metal heteroatom bond strengths, especially for late-transition-metal complexes. To understand metal carbon bonding, Jones and co-workers have compared Rh−C bond strengths[21] to hydrocarbon H−C bond strengths. A similar experimental study conducted by Wolczanski and co-workers compared Ti−C and H−C bonding.[22] It was found that M−C bond strengths correlate with H−C bond strengths with a slope of ∼1.2, which indicates that there are larger differences in M−C bond enthalpies for a single metal fragment compared with H−C bond enthalpy differences.

On the theoretical side, Perutz, Eisenstein, and co-workers used BP86 and B3PW91 density functionals to evaluate M−C/H−C bond enthalpy correlations.[23] Both of these functionals showed high correlation between computed H−C bond dissociation enthalpies and experimental bond dissociation enthalpies. The computed hydrocarbon bond dissociation enthalpies were then correlated with computed bond dissociation enthalpies for model complexes of the Jones (Tp′)Rh(H)($CNCH_2CMe_3$)(R) and Wolczanski (*t*-Bu_3SiO)$_2$Ti(NHSi*t*-Bu_3)(R) systems where R = hydrocarbyl. The B3PW91 and BP86 functional correlations between computed H−C and M−C bond dissociation enthalpies gave high linear correlations with slopes close to those found experimentally. This analysis by Perutz, Eisenstein, and co-workers showed that density functional methods can be used to accurately evaluate relative bond enthalpy relationships between H−C and M−C bonds.

Energy decomposition analysis on the Rh−C and Ti−C bonds by Mitoraj et al. showed that radical stabilization energies control allyl and aryl M−C type bond strengths while orbital interactions control metal alkyl bond strengths.[24] Mitoraj et al. also noted that H−C and M−C bonds have different amounts of ionic versus covalent character.[24] Siegbahn has discussed trends in M−C bond strengths with a focus on the degree of ionic character.[25] Also, Harvey has related the strength of M−C bonds to partial carbanionic character speculating that steric influences are less important.[26]

Although there are several theoretical investigations of M−C bonding, there are only a few reports that have analyzed late-transition-metal heteroatom bonding. Most germane is the

dx.doi.org/10.1021/ic300350k | Inorg. Chem. 2012, 51, 6710−6718

early work by Ziegler and Baerends who used the Hartree−Fock−Slater (Xα) scheme to examine the bond energies for Ti−X, Zr−X, and Hf−X complexes compared with $(CO)_4$Co-(X).[27] They concluded that the Co−X bonds are weaker than corresponding Ti−X, Zr−X, or Hf−X bonds because of repulsive d_π-p_π interactions. However, there was no extensive comparison of cobalt alkyl versus cobalt heteroatom bonds. Landis and co-workers have used the B3LYP functional and ab initio methods to evaluate "valency-saturated" H_nM-X bond enthalpies.[28] They found that the general bond enthalpy ordering consisted of X = NH_2 < OH < F. However, early transition-metal complexes showed trends consistent with metal electronegativity while late-transition-metal bond enthalpies did not. Comparison of relative metal heteroatom bond enthalpies to metal alkyl bond enthalpies showed some correlation to the difference in natural electronegativities. In conclusion, Landis and co-workers stated that late-transition-metal bond enthalpies have a "complex interplay between bond polarity and lone pair interactions."[28]

COMPUTATIONAL METHODOLOGY

All stationary points were confirmed as minima by full calculation of the Hessian. Only the lowest energy minima are reported. (U)BP86/6-31G(d,p)[LANL2DZ] optimizations were carried out in Gaussian 09.[29] This level of theory provides accurate estimates of bond dissociation enthalpies compared to experiment for H−C and Rh/Ti−C bonds.[23] For our own benchmarking purposes, in the Results and Discussion section, we compare CCSD(T) M−X bond dissociation energies with BP86 values. However, we note that the extremely high computational cost of carrying out CCSD(T) calculations limited us to using the 6-31G(d,p)[LANL2DZ] basis set. Although chemically accurate values are expected only with a very large basis set for correlated ab initio methods, this basis set is expected to provide accurate relative bond energies.

Bond energy decomposition analysis (EDA) was carried out using the Amsterdam Density Functional (ADF) package.[30] Energy decomposition analysis was performed using the BP86 functional in conjunction with Slater-type orbital triple ξ quality TZ basis set with polarization functions (TZP). The zero-order regular approximation (ZORA) was also utilized. As discussed by Bickelhaupt and Baerends,[31] the ADF energy decomposition analysis follows the classic Morokuma-type/Ziegler-Rauk[32] approach within the Kohn−Sham molecular orbital formalism.[33] In this form the bond dissociation energy of a molecule, for example A−B, results from two terms (eq 3 and Scheme 3). The first energy term is the geometrical distortion energy (ΔE_{dist}). This is the energy penalty required to transform relaxed radical fragments with wave functions $\Psi^0{}_A$ and $\Psi^0{}_B$ into geometries and wave functions Ψ_A and Ψ_B properly prepared for bonding but at an infinite and noninteracting distance. The second energy term in eq 3 is the interaction energy (ΔE_{int}) between distorted radical fragments. The interaction energy, which is the same as the bond energy (BE), is dissected into three physical components (eq 4): (1) electrostatic energy (ΔE_{es}), which is the result of overlapping frozen (unrelaxed) fragment electron densities ($\Psi_A\Psi_B$) and includes nuclei−nuclei, nuclei-electron, and electron−electron quasiclassical Coulombic interactions (eq 5). (2) Pauli repulsion (ΔE_{Pauli}), which is the energy change upon antisymmetrization and renormalization of the overlapped fragment densities, $\Psi^0 = N\hat{A}\{\Psi_A\Psi_B\}$ (eq 6). (3) Orbital stabilization (ΔE_{orb}), that is composed of inter- and intramolecular charge transfer interactions, is provided by a comparison of the antisymmetrized DFT wave function with the fully relaxed energy (eq 7). For the A−B bond the ΔE_{orb} term is mainly the result of stabilization gained from the combination of singly occupied orbitals of radical fragments A and B along with a smaller contribution from the interaction of doubly occupied orbitals on one fragment with empty orbitals on the other fragment.

$$-\mathrm{BDE} = \Delta E_{dist} + \Delta E_{int} \quad (3)$$

Scheme 3. Pictorial Representation of the Steps Involved in Energy Decomposition Analysis

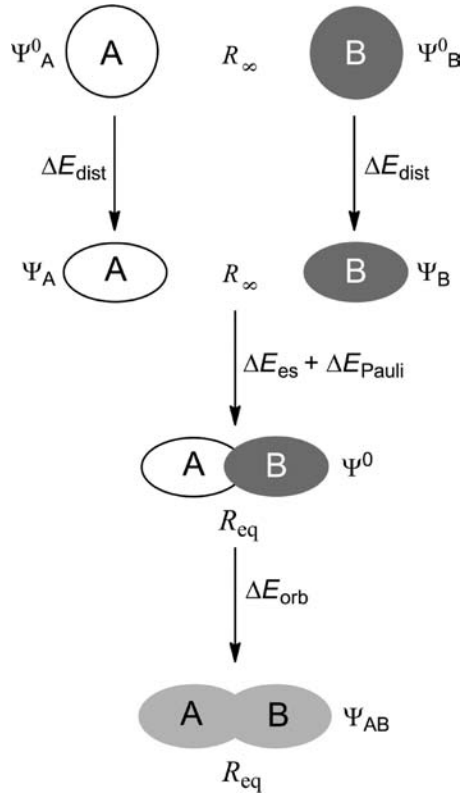

$$-\mathrm{BE} = \Delta E_{int} = \Delta E_{es} + \Delta E_{Pauli} + \Delta E_{orb} \quad (4)$$

$$\Delta E_{es} = \sum_{\substack{\alpha\in A\\ \beta\in B}} \frac{Z_\alpha Z_\beta}{R_{\alpha\beta}} + \sum_{\alpha\in A}\int \frac{\rho_B(r)Z_\alpha}{|R_\alpha - r|}dr + \sum_{\beta\in B}\int \frac{\rho_A(r)Z_\beta}{|R_\beta - r|}dr + \int \frac{\rho_A(r_1)\rho_B(r_2)}{r_{12}}dr_1dr_2 \quad (\mathrm{eq5})$$

$$\Delta E_{Pauli} = E^0 - (E_A + E_B) + \Delta E_{XC} \quad (6)$$

$$\Delta E_{orb} = E_{AB} - E^0 \quad (7)$$

The six systems studied (Scheme 2) were chosen because they include second- and third-row transition metal centers that span groups 8−10 on the periodic table.[2,5,8,16,34,35] This diverse set of metal ligand complexes was chosen so that trends identified in M−X bonds would be independent of the precise metal and ligand combination. Analysis of bond dissociation energies was performed on the hydrocarbon ligands methyl, ethyl, isopropyl, *tert*-butyl, benzyl, vinyl, and phenyl. The NR_2 ligands analyzed include NH_2, NHMe, NMe_2, NHPh, NPh_2, and NMePh. The alkoxide ligands studied include OH, OMe, and OPh. Fluoride ligand was also evaluated. Energy decomposition analysis was performed on the methyl, amido, hydroxo, and fluoride complexes.

RESULTS AND DISCUSSION

Comparison of Density Functional Theory to CCSD(T).

Density functional methods provide a computationally low-cost platform to analyze bond dissociation energies. However, there are several reports of known errors for common pure and hybrid functionals when evaluating bond dissociation energies.[36] As discussed in the background section, Perutz, Eisenstein, and co-workers utilized the BP86 functional

dx.doi.org/10.1021/ic300350k | Inorg. Chem. 2012, 51, 6710−6718

successfully to evaluate trends for Ti−C and Rh−C bond dissociation enthalpies.[23] However, there is a general lack of density functional benchmark studies for organometallic reactions.[37] Noteworthy is the work of Girolami, Dunning, and co-workers that compares chemically accurate correlated ab initio calculations with density functional methods for metal alkyl hydrides and the corresponding alkane complexes.[38] We have also compared CCSD(T) and BP86 bond energies and bond dissociation energies to establish whether this functional is sufficient to model the trends in bond energies for metal alkyl, amido, hydroxo, and fluoro type bonds.

The $(PMe_3)_2Rh(C_2H_4)(X)$ (**4−X**) and $CpRu(PH_3)_2(X)$ (a truncated version of **2−X**) complexes were chosen for comparative analysis because they were tractable with CCSD(T) theory. Table 1 gives the BEs and the bond dissociation energies (BDEs) for X = CH_3, NH_2, OH, and F. BEs differ from BDEs in that they do not include radical fragment relaxation. BP86 overestimates the BEs and BDEs by an average of ∼3 kcal/mol for the $(PMe_3)_2Rh(C_2H_4)(X)$ complexes and ∼4 kcal/mol for the $CpRu(PH_3)_2(X)$ complexes compared to the highly accurate CCSD(T) theory. The discrepancy between BP86 and CCSD(T) becomes larger as the M−X bond becomes more polarized from X = CH_3 to X = F. For example, the BDE energy difference between BP86 and CCSD(T) is less than 1 kcal/mol for M−CH_3 bonds but up to 8 kcal/mol different for the M−F bonds. The values in Table 1 show that although BP86 does not provide absolute accuracy compared with CCSD(T) it does provide a reasonable choice to evaluate bonding trends.

Table 1. Comparison of (U)CCSD(T)//(U)BP86 and (U)BP86 Bond Dissociation Energies and Bond Energies[a] (in parentheses) with the 6-31G(d,p)[LANL2DZ] Basis Set (in kcal/mol)[b]

	$(PMe_3)_2Rh(C_2H_4)(X)$		$Cp(PH_3)_2Ru(X)$	
X	(U)CCSD(T)	(U)BP86	(U)CCSD(T)	(U)BP86
CH_3	52.8 (66.7)	51.9 (67.2)	56.3	57.0
NH_2	59.5 (66.0)	61.3 (68.8)	55.3	57.8
OH	78.2 (86.7)	81.5 (90.2)	67.8	73.3
F	105.8 (116.5)	112.0 (122.0)	91.6	100.4
MUE		2.6 (3.1)		4.3

[a]M−X bond energies do not include radical fragment geometry relaxation. [b]MUE = mean unsigned error.

Trends in Computed Bond Energies and Bond Dissociation Energies. Table 2 gives the BP86 bond dissociation energies and bond energies for complexes **1−X** through **6−X**.[39] Figures 1 and 2 show the plotted BDEs and BEs. The BDE values for Ir(III) complex **6−X** are on average strongest while Ru(II) complexes **2−X** and **3−X** have the weakest bonds. There is a clear trend in progressively larger BDE values along the series from methyl to fluoride ligands for all of the complexes studied. The trend is not perfectly monotonic, mainly because of the methyl species.

Figure 2 shows plots of the bond energies, which excludes metal and X group fragment relaxation energy, versus ligand identity. The major difference between Figures 1 and 2 is that in Figure 2 M−CH_3 bond energies are larger than the corresponding M−NH_2 bonds, while Figure 1 shows that M−CH_3 bond dissociation energies are smaller than M−NH_2 bond dissociation energies. The larger M−CH_3 bond energies are due to the larger methyl radical relaxation energy corresponding to the change from a tetrahedral species to a planar methyl radical compared with the smaller NH_2 radical relaxation energy. There is also metal fragment relaxation energy, but this energy is small and nearly constant throughout the series from X = CH_3 to F. On average the radical relaxation energy for the metal alkyl species is 11.8 kcal/mol whereas for amido, hydroxo, and fluoride complexes the relaxation energies are 4−8 kcal/mol less.

The greater bond energy for M−CH_3 relative to M−NH_2 suggests the possibility of d_π-p_π repulsions that destabilize the M−NH_2 bond. However, this requires that multiple lone pairs associated with M−OH and M−F bonds to either have a diminished destabilizing effect or be counterbalanced by other forces since the bond energies monotonically increase in strength along the series M−NH_2 to M−OH to M−F.

Table 2. (U)BP86/6-31G(d,p)[LANL2DZ] Bond Dissociation Energies and Bond Energies[a] for Complexes 1−X through 6−X (kcal/mol)

X	1−X	2−X	3−X	4−X	5−X	6−X
			Bond Dissociation Energies			
CH_3	66.9	54.7	51.8	51.9	61.7	71.5
NH_2	70.2	59.3	60.0	61.3	67.6	71.3
OH	83.8	78.7	81.9	81.5	84.4	87.7
F	111.5	110.0	116.9	112.0	114.1	112.6
			Bond Energies			
CH_3	76.0	66.3	64.0	67.2	70.4	79.8
NH_2	72.5	63.1	63.1	68.8	70.8	73.5
OH	86.5	84.7	88.6	90.2	88.6	92.1
F	114.6	118.4	129.0	122.0	119.9	118.5

[a]M−X bond energies do not include radical fragment geometry relaxation.

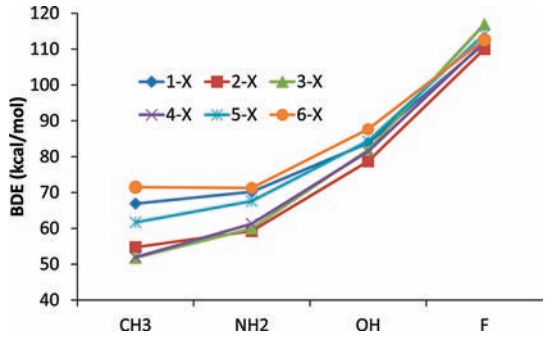

Figure 1. Plot of bond dissociation energies (kcal/mol) as a function of X group (CH_3, NH_2, OH, F) for complexes **1−X** through **6−X**.

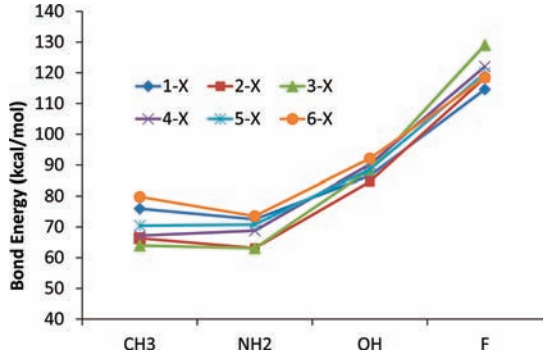

Figure 2. Plot of bond energies (kcal/mol) as a function of X group (CH_3, NH_2, OH, F) for complexes **1−X** through **6−X**.

dx.doi.org/10.1021/ic300350k | Inorg. Chem. 2012, 51, 6710−6718

To examine the chemical and physical origin of these bonding trends we have carried out energy decomposition analysis (EDA) on a series of complexes to dissect the bond energy (ΔE_{int}) into electrostatic (ΔE_{es}), closed-shell repulsion (ΔE_{Pauli}), and orbital stabilization energies (ΔE_{orb}). Table 3 gives the BP86/TZP homolytic (M−X → M$^{\bullet}$ + X$^{\bullet}$) partitioned bond energies for complexes **1−X**.

Table 3. BP86/TZP Energy Decomposition Analysis for Pt−X Bonds of Complex (DMPE)Pt(CH_3)(X) (1−X)[a]

1−X	ΔE_{int}	ΔE_{Pauli}	ΔE_{es}	ΔE_{orb}	r(Pt−X)
1−CH_3	−71.4	157.9	−120.3	−109.0	2.108
1−NH_2	−67.4	176.9	−115.0	−129.4	2.060
1−OH	−83.3	136.2	−77.4	−142.2	2.042
1−F	−114.5	145.2	−77.4	−182.4	2.014

[a]Energies are reported in kcal/mol. Pt−X distances are given in angstroms.

The total Pt−C bond energy in **1−CH_3** (DMPE)Pt(CH_3)$_2$ is −71.4 kcal/mol. This bond energy is composed of −120.3 kcal/mol of stabilization resulting from overlapping frozen electron densities for the electrostatic interactions and −109.0 kcal/mol of orbital stabilization resulting from the interaction of the Pt and methyl fragment singly occupied orbitals as well as filled-empty interactions between fragments. Also contributing to the Pt−C bond energy is 157.9 kcal/mol of destabilization resulting from the Pauli repulsion between the methyl fragment with the occupied metal d-orbital electrons and the Pt ligands.

The Pt−N bond (ΔE_{int} = −67.4 kcal/mol) in **1−NH_2** (DMPE)Pt(CH_3)(NH_2) is 4.0 kcal/mol weaker than the Pt−C bond in **1−CH_3**. This weaker bond is mainly the result of 19.0 kcal/mol more destabilizing Pauli repulsion as well as 5.3 kcal/mol less stabilizing electrostatic interactions. Offsetting most of the Pauli repulsion is the orbital stabilization, which is 20.4 kcal/mol more stabilizing in **1−NH_2** than in **1−CH_3**. The increase in Pauli repulsion can be attributed to the shorter Pt−N bond distance of 2.06 Å compared to the Pt−C distance of 2.10 Å. Analysis of **1−NH_2** with the Pt−N bond distance stretched to 2.10 Å results in only a 0.7 kcal/mol increase in ΔE_{int}, but ΔE_{Pauli} drops to a value of 157.4 kcal/mol from a value of 176.9 kcal/mol in the optimized structure. The ΔE_{Pauli} value for the stretched Pt−N bond is almost identical to the ΔE_{Pauli} value in **1−CH_3**. Pt−N bond elongation also decreases ΔE_{es} and ΔE_{orb} by 12.0 and 6.8 kcal/mol, respectively.

The Pt−O bond energy in **1−OH** is −83.3 kcal/mol. This bond energy is 11.9 and 15.9 kcal/mol larger than the Pt−C and Pt−N bond energies in **1−CH_3** and **1−NH_2**, respectively. This increase in Pt−X bond energy is not due to an increase in electrostatic interactions from the shorter Pt−X bond distance (Pt−O = 2.04 Å). The ΔE_{es} term for **1-OH** is −77.4 kcal/mol, which is 42.9 kcal/mol less stabilizing than the ΔE_{es} term in **1−CH_3**. Rather, the stronger Pt−OH bond is the result of two effects. First, the ΔE_{Pauli} term in **1-OH** is 21.7 kcal/mol *less* destabilizing compared to the ΔE_{Pauli} term in **1−CH_3** and 40.7 kcal/mol *less* destabilizing compared to the ΔE_{Pauli} term in **1−NH_2**. Second, the stronger Pt−OH bond arises from a substantial increase in orbital stabilization energy. The ΔE_{orb} value in **1-OH** is −142.2 kcal/mol, which is 33.2 kcal/mol more stabilizing than in complex **1−CH_3** and 12.7 kcal/mol more stabilizing than in complex **1−NH_2**.

The Pt−F (2.01 Å) bond energy in **1−F** is −114.5 kcal/mol. The Pauli repulsion in this bond (ΔE_{Pauli} = 145.2 kcal/mol) is larger relative to the Pauli repulsion in the Pt−OH bond of complex **1-OH** but is smaller than the Pauli repulsion in the Pt−C and Pt−N bonds of complexes **1−CH_3** and **1−NH_2**. The origin of the large Pt−F bond energy is due to the orbital interaction energy that is −182.4 kcal/mol stabilizing, which is 73.4 kcal/mol more stabilizing than the orbital interactions in the Pt−C bond energy of complex **1−CH_3**.

It is interesting to note that for the Pt−C and Pt−N bonds orbital stabilization is less than the Pauli repulsion and therefore requires electrostatic interactions for the Pt and X fragments to be bound. In contrast, for the Pt−O and Pt−F bonds the orbital stabilization energy is larger than the Pauli repulsion energy.

Overall, the EDA results for complexes **1−X** reveal that orbital interactions consistently increase in stabilization along the series Pt−C, Pt−N, Pt−O, to Pt−F. In contrast, the Pauli repulsion fluctuates along this series. Therefore, a straightforward bonding modeling emerges based on orbital stabilization that can be readily rationalized by the impact of electronegativity on the X ligand fragment orbital energies. Figure 3

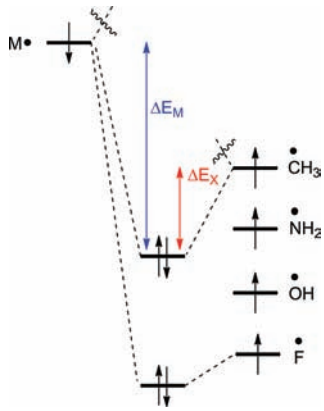

Figure 3. Qualitative model for M−X bond orbital stabilization.

shows that the orbital stabilization that occurs in M−X bonds is due to stabilization of both the neutral metal radical fragment (ΔE_M) and the neutral ligand radical fragment (ΔE_X) mainly because of the bonding interaction of the singly occupied orbitals. For all of these bonds, the X fragment radical is more electronegative than the metal fragment radical and therefore the majority of orbital stabilization results from ΔE_M. When the methyl radical is changed to a more electronegative fragment the M and X orbital energy gap increases. This has the effect of decreasing the ΔE_X stabilization energy while substantially increasing the ΔE_M stabilization energy, due to delocalization of the metal fragment electron onto the X fragment, leading to greater overall orbital stabilization.

It is important to recognize that this EDA is a molecular orbital type method. The increase in Pt−X bond stabilization along the series CH_3 to F is manifested as charge transfer that results from singly occupied orbitals overlapping, as well as a smaller contribution from doubly occupied to unoccupied orbital interactions, and not electrostatic stabilization. In fact, as noted above the ΔE_{es} term decreases along the CH_3, NH_2, OH, F series. A similar trend was computed by Ziegler et al. for $(CO)_4Co(X)$ complexes where X = CH_3, NH_2, and OH.[27b] The EDA electrostatic term is a combination of classic nuclear−nuclear repulsion, quasiclassical nuclear-electron attraction, and quasiclassical electron−electron repulsion.

dx.doi.org/10.1021/ic300350k | *Inorg. Chem.* 2012, 51, 6710−6718

Although the more electronegative fluorine induces larger nuclear-electron stabilizing attraction with the Pt radical fragment than the less electronegative methyl fragment, this stabilization is not enough to compensate for the increase in nuclear−nuclear repulsion between the Pt fragment and the F nuclei.[33b] It is also important to realize that these EDA results, and the EDA results for HX bonds discussed later, do not conflict with a valence bond viewpoint where strong polar-covalent bonds are the result of an increase in ionic M^+X^- valence bond weighting and greater covalent-ionic resonance stabilization.[40,41]

For the Ru(II) complexes **2−X**, $Cp^*Ru(PMe_3)_2(X)$, a slightly different story emerges from the EDA. Table 4 gives the dissected bond energies for complexes **2−X**. Again, similar to complexes **1−X**, the orbital interaction energies provide a model for the increase in bond strength as the methyl ligand is changed along the series amido, hydroxo, to fluoride. The ΔE_{orb} value in **2−CH$_3$** is −102.3 kcal/mol. The orbital stabilization increases to −112.1, −132.0, and −169.9 kcal/mol for complexes **2−NH$_2$**, **2−OH**, 2−F, respectively. In contrast to the **1−X** complexes, the ΔE_{Pauli} values in the **2−X** complexes continually decrease and become less destabilizing along this alkyl and heteroatom ligand series. The ΔE_{Pauli} term is 139.9 kcal/mol destabilizing in **2−CH$_3$** and drops by 2.3 to 137.6 kcal/mol for the Ru−N bond in complex **2−NH$_2$**. It further drops to 118.8 kcal/mol and then to 111.6 kcal/mol in complexes **2−OH** and **2−F**.

Table 4. BP86/TZP Energy Decomposition Analysis for Ru−X Bonds of Complex $Cp^*Ru(PMe_3)_2(X)$ (2−X)[a]

2−X	ΔE_{int}	ΔE_{Pauli}	ΔE_{es}	ΔE_{orb}	r(Ru−X)
2−CH$_3$	−65.1	139.9	−102.6	−102.3	2.162
2−NH$_2$	−61.0	137.6	−86.5	−112.1	2.187
2−OH	−81.9	118.8	−68.6	−132.0	2.144
2−F	−115.9	111.6	−57.6	−169.9	2.103

[a]Energies are reported in kcal/mol. Ru−X distances are given in angstroms.

The change in Pauli repulsion means that the Ru−N bond energy in **2−NH$_2$**, which is 4.1 kcal/mol less than the Ru−C bond energy in **2−CH$_3$**, cannot be rationalized based on increased closed-shell repulsion, which includes d_π-p_π repulsion. Rather, the orbital interaction stabilization that increases by 9.8 kcal/mol is not significant enough to compensate for the drop in electrostatic stabilization. Similar to complexes **1−X**, there is a continual drop in electrostatic stabilization along the alkyl and heteroatom ligand series for complexes **2−X**.

Table 5 gives the BP86/TZP EDA values for complexes **3−X** through **6−X**. Inspection of the EDA data reveals that complexes **3−X** have trends very similar to complexes **2−X**, which is due to the common Ru(II) metal center. Complexes **4−X**, **5−X**, and **6−X** have trends similar to complexes **1−X**. Again, orbital stabilization provides a straightforward bonding model for the bond energy trends in all of these complexes.

Correlation between M−X and H−X Bond Energies. As discussed in the introduction, the studies of Bryndza, Bercaw, Jones, and Wolczanski have resulted in the clear conclusion that M−X and H−X bond energies can be correlated. Although Eisenstein analyzed M−C versus H−C bonds, there was no comparison across a set of hydrocarbon and heteroatom M−X bond energies. For complexes **1−X**, **2−X**, **4−X**, and **6−X** we have computed the bond dissociation energies for 17 different X groups (see Table 6 title). The energies and correlation plots are shown in the Supporting Information. Similar to the work of Perutz, Eisenstein, and co-workers, we find that the degree of linear correlation depends on the metal complex. Table 6 gives the linear regression lines for the correlation between M−X and H−X bond dissociation energies. For the Pt complex the slope is closest to unity at 1.2 and the R^2 value of 0.88 indicates a reasonable correlation. A similar analysis and result was reported by Landis and co-workers for metal hydrides.[28] The worst correlation was found for the $(PMe_3)_2Rh(C_2H_4)(X)$ complexes with an R^2 of only 0.74 and a slope of 1.3. The highest degree of linear correlation was found for *cis*-$(acac)_2Ir(Py)(X)$ with an R^2 value of 0.95.

Table 5. BP86/TZP Energy Decomposition Analysis for Complexes $(DMPE)_2Ru(H)(X)$ (3−X), $(PMe_3)_2Rh(C_2H_4)(X)$ (4−X), (Tp)(CO)Ru(Py)(X) (5−X), and *cis*-$(acac)_2IrPy(X)$ (6−X)[a]

M−X	ΔE_{int}	ΔE_{Pauli}	ΔE_{es}	ΔE_{orb}	r(M−X)
3−CH$_3$	−64.2	124.1	−90.5	−97.8	2.257
3−NH$_2$	−62.3	124.0	−77.8	−108.6	2.275
3−OH	−86.6	106.9	−62.9	−130.6	2.258
3−F	−125.9	96.5	−51.9	−170.4	2.251
4−CH$_3$	−65.8	136.2	−101.6	−100.3	2.117
4−NH$_2$	−67.2	155.3	−105.2	−117.3	2.038
4−OH	−89.1	131.2	−74.9	−145.4	2.047
4−F	−121.1	126.0	−65.6	−181.5	2.048
5−CH$_3$	−69.6	137.8	−104.1	−103.2	2.124
5−NH$_2$	−69.9	151.0	−98.6	−122.4	2.107
5−OH	−88.0	131.4	−75.2	−144.2	2.067
5−F	−119.1	122.8	−61.2	−180.6	2.017
6−CH$_3$	−75.7	169.8	−125.5	−120.0	2.070
6−NH$_2$	−68.3	180.3	−114.0	−134.6	2.041
6−OH	−87.2	145.5	−82.6	−150.1	2.026
6−F	−114.6	136.1	−66.6	−184.1	1.985

[a]Energies are reported in kcal/mol. M−X distances are given in angstroms.

Table 6. Linear Regression Analysis ($y = mx + b$) for Plots of M−X versus H−X Bond Dissociation Energies (kcal/mol)[a]

M−X	m	b	R^2
1−X	1.2	−70	0.88
2−X	1.5	−112	0.81
4−X[b]	1.3	−92	0.74
6−X	1.3	−76	0.95

[a]X = methyl, ethyl, isopropyl, *tert*-butyl, benzyl, vinyl, phenyl, NH_2, NHMe, NMe_2, NHPh, NPh_2, NMePh, OH, OMe, OPh, F. [b]When X = OPh is not analyzed, the correlation improves with an R^2 = 0.81.

Analysis of H−X Bonds. To understand the correlation between M−X and H−X bond energies, EDA was also performed on CH_4, NH_3, OH_2, and HF (Table 7). Comparison of the EDA terms in Table 7 versus those in Tables 3−5 indicates that the EDA terms for H−X bonds are generally larger than the EDA terms for M−X bonds because of the shorter H−X bond lengths.[41]

The methane H−C bond energy of −121.2 kcal/mol is composed of −141.4 and −56.8 kcal/mol of stabilization

dx.doi.org/10.1021/ic300350k | Inorg. Chem. 2012, 51, 6710−6718

Table 7. BP86/TZP Energy Decomposition Analysis for H−X Bonds[a]

	ΔE_{int}	ΔE_{Pauli}	ΔE_{es}	ΔE_{orb}	r(H−X)
CH_4	−121.2	77.1	−56.8	−141.4	1.100
NH_3	−117.1	175.7	−80.2	−212.6	1.028
H_2O	−127.5	175.7	−69.2	−233.9	0.974
HF	−144.2	182.0	−53.5	−272.7	0.933

[a]Energies are reported in kcal/mol. M−X distances given in angstroms.

resulting from orbital and electrostatic interactions and 77.1 kcal/mol of destabilizing Pauli repulsion.[42] The ammonia H−N bond energy (ΔE_{int} = −117.1 kcal/mol) is 4.1 kcal/mol weaker than the methane H−C bond and only after radical relaxation energy is accounted for does the ammonia bond dissociation energy increase by 2.1 kcal/mol relative to the methane bond dissociation energy.

In the ammonia H−N bond the Pauli repulsion energy increases by 98.6 kcal/mol compared to the Pauli repulsion in the H−C bond of methane. This Pauli repulsion is also much larger than the Pauli repulsion found in M−N bonds. For the H−N bond the Pauli repulsion between the hydrogen radical and the same spin electrons on the NH_2 radical fragment is highly repulsive because of the short bond length. Offsetting this increase in repulsion is a 71.1 kcal/mol larger orbital stabilization value compared with the orbital stabilization found in the H−C bond of methane. Different from the M−X bonding interactions, the electrostatic interactions in the H−N bond of ammonia becomes more stabilizing by 23.4 kcal/mol compared to the electrostatic interactions in the H−C bond of methane. However, the increase in orbital and electrostatic stabilization is not enough to compensate for the increase in Pauli repulsion.

Analysis of the ammonia H−N bond stretched to the methane H−C bond distance was also carried out. Stretching the H−N bond lowers the bond energy by 2.3 kcal/mol. Unlike the comparison carried out for M−C and M−N bonds, lengthening the ammonia H−N bond resulted in a Pauli repulsion energy that remains substantially greater than the methane Pauli repulsion energy by 66.6 kcal/mol. The electrostatic and orbital interactions for the stretched H−N bond of ammonia also remain significantly more stabilizing than for the H−C bond of methane by 16.1 and 44.1 kcal/mol, respectively.

The water H−O bond is 6.3 kcal/mol more stable than the methane H−C bond and 10.4 kcal/mol more stable than the H−N bond of ammonia. Similar to the ammonia H−N bond, the water H−O bond compared to the methane H−C bond shows an increase in both orbital and electrostatic stabilization with the orbital interaction being significantly more important. The Pauli repulsion energies for the H−O and H−N bonds are identical. The electrostatic stabilization decreases for the H−O bond compared with the H−N bond. This result highlights that the change in bond energy is the result of the orbital interactions that become more substantial and more stabilizing.

The H−F bond energy is 23 kcal/mol more stable than the C−H bond energy of methane. This difference can be directly attributed to the orbital interactions that increase by 131.3 kcal/mol because the electrostatic energy becomes 3.3 kcal/mol less stabilizing. The Pauli repulsion energy also increases by 104.9 kcal/mol in the H−F bond compared to the C−H bond energy of methane. Shaik et al. have labeled the H−F bond as an example of a charge-shift bond where the resonance interaction between the principal covalent valence bond wave function (H−F) and the ionic valence bond wave function (H^+F^-) accounts for most of the bonding.[40] In this MO EDA scheme the covalent-ionic resonance stabilization is manifested within the ΔE_{orb} term.

Since the trends in M−X bond energies follow orbital stabilization energies, we wondered if the ΔE_{orb} values for both M−X and H−X bonds could be correlated. Indeed, for the (DMPE)Pt(CH_3)(X) complexes the correlation has an R^2 value of 0.88 (Figure 4). The Cp*Ru(PMe_3)$_2$(X) also shows that the

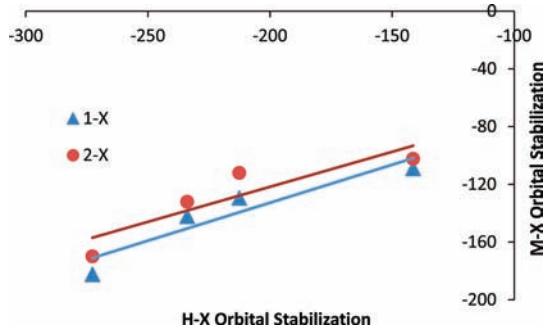

Figure 4. Correlation plot between M−X and H−X bond ΔE_{orb} stabilization energies (kcal/mol) for complexes **1**−**X** and **2**−**X**.

ΔE_{orb} values for both M−X and H−X bonds are also moderately correlated with an R^2 value of 0.80. The correlations produce slopes of ∼0.5. This indicates that the change in orbital interactions is larger for H−X bonds than for M−X bonds and therefore is not the origin of the slopes that are greater than 1 in Table 6 when M−X and H−X bond dissociation energies are correlated. Inspection of the EDA data reveals that the difference in Pauli repulsion and to a lesser extent the difference in electrostatic stabilization is the origin of the greater than 1 slope. In H−X bonds the Pauli repulsion significantly increases along the series from X = CH_3 to X = F whereas for M−X bond energies the Pauli repulsion fluctuates or decreases along this series. Again, this is the result of a shorter bond length in H−X bonds rather than the amount of electrons. In the H−X bonds there is significant Pauli repulsion between the hydrogen electron and the same spin electrons on X. In addition, for M−X bond energies there is a decrease in electrostatic stabilization along the X = CH_3 to F ligand series whereas in H−X bonds the electrostatic stabilization increases from methane to ammonia and then decreases in water and H−F.

CONCLUSION

Using energy decomposition calculations we have developed a straightforward model for relative M−X bond strengths based on orbital charge transfer stabilization along the alkyl to heteroatom ligand series (X = CH_3, NH_2, OH, F). We also found that Pauli repulsion, which includes closed-shell d_π-p_π repulsion, generally decreases along the alkyl to heteroatom ligand series and therefore does not control M−X bond strengths. However, Pauli repulsion does play an important role when comparing M−CH_3 and M−NH_2 bond energies for some of the complexes studied. It was also revealed that stabilizing electrostatic interactions generally decrease along the alkyl to heteroatom ligand series.

dx.doi.org/10.1021/ic300350k | Inorg. Chem. 2012, 51, 6710−6718

Correlation between M−X and H−X bond dissociation energies was found to be good. This correlation occurs because the orbital stabilization energies in both M−X and H−X bonds are a function of the orbital electronegativity of the X group. The greater than 1 slope when correlating M−X and H−X bond dissociation energies was traced back to differences in Pauli repulsion and electrostatic stabilization.

■ ASSOCIATED CONTENT

Supporting Information

Full references 29 and 30, absolute energies, *xyz* coordinates, correlation plots of MX/HX bond dissociation energies, heterolytic fragmentation energy decomposition analysis values. This material is available free of charge via the Internet at http://pubs.acs.org.

■ AUTHOR INFORMATION

Corresponding Author

*E-mail: dhe@chem.byu.edu.

Notes

The authors declare no competing financial interest.

[§]A contribution from the Center for Catalytic Hydrocarbon Functionalization, Energy Frontier Research Center.

■ ACKNOWLEDGMENTS

D.H.E. thanks Brigham Young University (BYU) and the Fulton Supercomputing Lab (FSL) for computational support. Acknowledgment is made to the Donors of the American Chemical Society Petroleum Research Fund for support to D.H.E (51081-DNI3). EDA analysis of bond energies was supported as part of the Center for Catalytic Hydrocarbon Functionalization, an Energy Frontier Research Center Funded by the U.S. Department of Energy, Office of Science, Office of Basic Energy Sciences, under Award Number DE-SC0001298. D.H.E. also thanks Mariusz Mitoraj for helpful discussions on bond energy decomposition strategies.

■ REFERENCES

(1) Bryndza, H. E.; Tam, W. *Chem. Rev.* **1988**, *88*, 1163.

(2) (a) Feng, Y.; Lail, M.; Barakat, K. A.; Cundari, T. R.; Gunnoe, T. B.; Petersen, J. L. *J. Am. Chem. Soc.* **2005**, *127*, 14174. (b) Feng, Y.; Lail, M.; Foley, N. A.; Gunnoe, T. B.; Barakat, K. A.; Cundari, T. R.; Petersen, J. L. *J. Am. Chem. Soc.* **2006**, *128*, 7982. (c) Foley, N. A.; Lail, M.; Lee, J. P.; Gunnoe, T. B.; Cundari, T. R.; Petersen, J. L. *J. Am. Chem. Soc.* **2007**, *129*, 6765. (d) Cundari, T. R.; Grimes, T. V.; Gunnoe, T. B. *J. Am. Chem. Soc.* **2007**, *129*, 13172.

(3) Conner, D.; Jayaprakash, K. N.; Cundari, T. R.; Gunnoe, T. B. *Organometallics* **2004**, *23*, 2724.

(4) Webb, J. R.; Pierpont, A. W.; Munro-Leighton, C.; Gunnoe, T. B.; Cundari, T. R.; Boyle, P. D. *J. Am. Chem. Soc.* **2010**, *132*, 4520.

(5) (a) Oxgaard, J.; Tenn, W. J., III; Nielsen, R. J.; Periana, R. A.; Goddard, W. A., III *Organometallics* **2007**, *26*, 1565. (b) Ess, D. H.; Bischof, S. M.; Oxgaard, J.; Periana, R. A.; Oxgaard, J.; Tenn, W. J., III; Nielsen, R. J.; Periana, R. A.; Goddard, W. A., III *Organometallics* **2008**, *27*, 6440. (c) Bischof, S. M.; Ess, D. H.; Meier, S. K.; Oxgaard, J.; Nielsen, R. J.; Bhalla, G.; Goddard, W. A., III; Periana, R. A. *Organometallics* **2010**, *29*, 742.

(6) (a) Kloek, S. M.; Heinekey, D. M.; Goldberg, K. I. *Angew. Chem., Int. Ed.* **2007**, *46*, 4736. (b) Hanson, S. K.; Heinekey, D. M.; Goldberg, K. I. *Organometallics* **2008**, *27*, 1454. (c) Luedtke, A. T.; Goldberg, K. I. *Angew. Chem., Int. Ed.* **2008**, *47*, 7694.

(7) (a) Williams, T. J.; Caffyn, A. J. M.; Hazari, N.; Oblad, P. F.; Labinger, J. A.; Bercaw, J. E. *J. Am. Chem. Soc.* **2008**, *130*, 2418. (b) Bercaw, J. E.; Hazari, N.; Labinger, J. A.; Oblad, P. F. *Angew. Chem., Int. Ed.* **2008**, *47*, 9941. (c) Bercaw, J. E.; Hazari, N.; Labinger, J. A. *J. Org. Chem.* **2008**, *73*, 8654. (d) Bercaw, J. E.; Hazari, N.; Labinger, J. A. *Organometallics* **2009**, *28*, 5489.

(8) (a) Bergman, R. G. *Polyhedron* **1995**, *14*, 3227. (b) Fulton, J. R.; Holland, A. W.; Fox, D. J.; Bergman, R. G. *Acc. Chem. Res.* **2002**, *35*, 44 and references therein.

(9) Ess, D. H.; Gunnoe, T. B.; Cundari, T. R.; Goddard, W. A., III; Periana, R. A. *Organometallics* **2010**, *29*, 6801.

(10) (a) Lichtenberger, D. L.; Brown, T. L. *J. Am. Chem. Soc.* **1978**, *100*, 366. (b) Davy, R. D.; Hall, M. B. *Inorg. Chem.* **1989**, *28*, 3524. (c) Riehl, J.-F.; Jean, Y.; Eisenstein, O.; Pélissier, M. *Organometallics* **1992**, *11*, 729. (d) Macgregor, S. A.; MacQueen, D. *Inorg. Chem.* **1999**, *38*, 4868.

(11) (a) Hartwig, J. F. In *Organotransition Metal Chemistry*; University Science Books: Sausalito, CA, 2010; Chapter 4, pp 148−149 and 178. (b) Crabtree, R. H. In *The Organometallic Chemistry of the Transition Metals*, 5th ed.; John Wiley & Sons: New York, 2009.

(12) Caulton, K. G. *New J. Chem.* **1994**, *18*, 25.

(13) (a) Reinhold, M.; McGrady, J. E.; Perutz, R. N. *J. Am. Chem. Soc.* **2004**, *126*, 5268. (b) Nova, A.; Erhardt, S.; Jasmin, N.; Perutz, R. N.; Macgregor, S. A.; McGrady, J. E. *J. Am. Chem. Soc.* **2008**, *130*, 15499. (c) Nova, A.; Reinhold, M.; Perutz, R. N.; Macgregor, S. A.; McGrady, J. E. *Organometallics* **2010**, *29*, 1824. (d) Clot, E.; Eisenstein, O.; Jasim, N.; Macgregor, S. A.; McGrady, J. E.; Perutz, R. N. *Acc. Chem. Res.* **2011**, *44*, 333.

(14) Mayer, J. M. *Comments Inorg. Chem.* **1988**, *8*, 125.

(15) Holland, P. L.; Andersen, R. A.; Bergman, R. G. *Comments Inorg. Chem.* **1999**, *21*, 115.

(16) (a) Bryndza, H. E.; Fong, L. K.; Paciello, R. A.; Tam, W.; Bercaw, J. E. *J. Am. Chem. Soc.* **1987**, *109*, 1444. (b) Bryndza, H. E.; Domaille, P. J.; Tam, W.; Fong, L. K.; Paciello, R. A.; Bercaw, J. E. *Polyhedron* **1988**, *7*, 1441. (c) Bulls, A. R.; Bercaw, J. E.; Manriquez, J. M.; Thompson, M. E. *Polyhedron* **1988**, *7*, 1409.

(17) (a) Stoutland, P. O.; Bergman, R. G.; Nolan, S. P.; Hoff, C. D. *Polyhedron* **1988**, *7*, 1429. (b) Holland, P. L.; Andersen, R. A.; Bergman, R. G.; Huang, J. K.; Nolan, S. P. *J. Am. Chem. Soc.* **1997**, *119*, 12800.

(18) See reference 11a pages 148−149 and 178.

(19) The word "bond energy" is used to mean the energy required to separate the M−X or H−X bond into radical fragments *without* geometry relaxation. This is different than bond dissociation energy that involves geometry relaxation of radical fragments.

(20) For a review see: Martinho Simões, J. A.; Beauchamp, J. L. *Chem. Rev.* **1990**, *90*, 629 and references therein.

(21) (a) Jones, W. D.; Hessell, E. T. *J. Am. Chem. Soc.* **1993**, *115*, 554. (b) Wick, D. D.; Jones, W. D. *Organometallics* **1999**, *18*, 495.

(22) (a) Bennett, J. L.; Wolczanski, P. T. *J. Am. Chem. Soc.* **1994**, *116*, 2179. (b) Bennett, J. L.; Wolczanski, P. T. *J. Am. Chem. Soc.* **1997**, *119*, 10696.

(23) (a) Clot, E.; Besora, M.; Maseras, F.; Mégret, C.; Eisenstein, O.; Oelckers, B.; Perutz, R. N. *Chem. Commun.* **2003**, 490. (b) Clot, E.; Mégret, C.; Eisenstein, O.; Perutz, R. N. *J. Am. Chem. Soc.* **2006**, *128*, 8350. (c) Evans, M. E.; Burke, C. L.; Yaibuathes, S.; Clot, E.; Eisenstein, O.; Jones, W. D. *J. Am. Chem. Soc.* **2009**, *131*, 13464.

(24) Mitoraj, M.; Zhu, H.; Michalak, A.; Ziegler, T. *Organometallics* **2007**, *26*, 1627.

(25) (a) Siegbahn, P. E. M. *J. Am. Chem. Soc.* **1994**, *116*, 7722. (b) Siegbahn, P. E. M. *J. Phys. Chem.* **1995**, *99*, 12723.

(26) Harvey, J. N. *Organometallics* **2001**, *20*, 4887.

(27) (a) Ziegler, T.; Tschinke, V.; Becke, A. *J. Am. Chem. Soc.* **1987**, *109*, 1351. (b) Ziegler, T.; Txchinke, V.; Versluis, L.; Baerands, E. J.; Ravenek, W. *Polyhedron* **1988**, *7*, 1625. (c) Ziegler, T.; Cheng, W.; Baerends, E. J.; Ravenek, W. *Inorg. Chem.* **1988**, *27*, 3458.

(28) Uddin, J.; Morales, C. M.; Maynard, J. H.; Landis, C. R. *Organometallics* **2006**, *25*, 5566.

(29) Frisch, M. J. et al. *Gaussian 09*, revision A.02; Gaussian, Inc.: Wallingford, CT, 2009.

(30) (a) Baerends, E. J.; et al. *ADF2010.02*; SCM, Theoretical Chemistry, Vrije Universiteit: Amsterdam, The Netherlands, 2007. (b) te Velde, G.; Bickelhaupt, F. M.; Baerends, E. J.; Fonseca Guerra,

C.; van Gisbergen, S. J. A.; Snijders, J. G.; Ziegler, T. *J. Comput. Chem.* **2001**, *22*, 931.
(31) Bickelhaupt, F. M.; Baerends, E. J. Kohn-Sham DFT: Predicting and Understanding Chemistry. In *Reviews in Computational Chemistry*; Boyd, D.B., Lipkowitz, K.B., Eds.; Wiley-VCH: New York, 2000; pp 1−86.
(32) Ziegler, T.; Rauk, A. *Theor. Chim. Acta* **1977**, *46*, 1.
(33) (a) Hopffgarten, M. v.; Frenking, G. *WIREs Comput. Mol. Sci.* **2012**, *2*, 43. (b) Krapp, A.; Bickelhaupt, F. M.; Frenking, G. *Chem.—Eur. J.* **2006**, *12*, 9196. (c) Lein, M.; Szabo, A.; Kovacs, A.; Frenking, G. *Faraday Discuss.* **2003**, *124*, 365.
(34) (a) Kaplan, A. W.; Bergman, R. G. *Organometallics* **1998**, *17*, 5072. (b) Hartwig, J. F.; Andersen, R. A.; Bergman, R. G. *Organometallics* **1991**, *10*, 1875. (c) Burn, M. J.; Fickes, M. G.; Hartwig, J. F.; Hollander, F. J.; Bergman, R. G. *J. Am. Chem. Soc.* **1993**, *115*, 5875. (d) Burn, M. J.; Fickes, M. G.; Hollander, F. J.; Bergman, R. G. *Organometallics* **1995**, *14*, 137. (e) Fulton, J. R.; Bouwkamp, M. W.; Bergman, R. G. *J. Am. Chem. Soc.* **2000**, *122*, 8799.
(35) Tye, J. W.; Hartwig, J. F. *J. Am. Chem. Soc.* **2009**, *131*, 14703.
(36) (a) Redfern, P. C.; Zapol, P.; Curtiss, L. A.; Raghavachari, K. *J. Phys.Chem. A* **2000**, *104*, 5850. (b) Grimme, S. *Angew. Chem., Int. Ed.* **2006**, *45*, 4460. (c) Wodrich, M. D.; Jana, D. F.; Schleyer, P. v. R.; Corminboeuf, C. *J. Phys. Chem. A* **2008**, *112*, 11495. (d) Steinmann, S. N.; Csonka, G.; Corminboeuf, C. *J. Chem. Theory Comput.* **2009**, *5*, 2950. (e) Song, S.; Tsuneda, T.; Sato, T.; Hirao, K. *Org. Lett.* **2010**, *12*, 1440. (f) Grimme, S. *Org. Lett.* **2010**, *12*, 4670. (g) Schwabe, T.; Huenerbein, R.; Grimme, S. *Synlett* **2010**, *10*, 1431. (h) Steinmann, S. N.; Corminboeuf, C. *J. Chem. Theory Comput.* **2010**, *6*, 1990.
(37) Quintal, M. M.; Karton, A.; Iron, M. A.; Boese, A. D.; Martin, J. M. *J. Phys. Chem. A* **2006**, *110*, 709.
(38) Flener-Lovitt, C.; Woon, D. E.; Dunning, T. H., Jr.; Girolami, G. S. *J. Phys. Chem. A* **2010**, *114*, 1843.
(39) The bond dissociation energies for a model of complex **1−X** was previously calculated. See: Macgregor, S. A.; Neave, G. W.; Smith, C. *Faraday Discuss.* **2003**, *124*, 111.
(40) For a recent perspective on VB theory see: Shaik, S.; Danovich, D.; Wu, W.; Hiberty, P. C. *Nat. Chem.* **2009**, *1*, 443.
(41) See the Supporting Information for a more detailed discussion on MO EDA electrostatic term and valence bond theory of polar covalent bonds.
(42) Mitoraj, M.; Zhu, H.; Michalak, A.; Ziegler, T. *J. Org. Chem.* **2006**, *71*, 9208.